

## Supporting Information

### Plasma-Induced Reconstruction of FeNi Alloy Nanoparticles on Carbon Nanotubes toward Highly Efficient OER

Xiao-Qing Deng<sup>a</sup>, Ying-Xin Luo<sup>a</sup>, Hao-Chen Yang<sup>b</sup>, Xiang Li<sup>c</sup>, Hao-Yu Lian<sup>b,\*</sup>

a. School of Architecture and Environment Art, Shanghai Urban Construction Vocational College,  
Shanghai 201415, China

b. School of Electrical and Information Engineering, Zhengzhou University, Zhengzhou 450001,  
China

c. School of Resources and Environmental Engineering, Shanghai Polytechnic University,  
Shanghai 201209, China

#### 1. Experimental

##### 1.1 Synthesis of FeNi/CNTs

The FeNi-CNTs catalysts were synthesized via a high-temperature pyrolysis method. In a typical procedure, 7.0 g of iron porphyrin and 1.0 g of carbon nanotubes (CNTs) were thoroughly mixed with different amounts of nickel nitrate precursor (0.5, 1.0, 1.5, and 2.0 g) to obtain homogeneous mixtures. The resulting mixtures were then transferred into alumina crucibles and subjected to thermal treatment at 900 °C for 2 h under an inert atmosphere, ensuring complete decomposition of the metal precursors and the formation of FeNi alloy nanoparticles. After naturally cooling to room temperature, a series of FeNi-CNTs catalysts were obtained and denoted as FeNi-CNTs-m, where m represents the mass (g) of nickel nitrate added during the synthesis.

##### 1.2 Preparation of FeNi/CNTs

Plasma modification of the FeNi-CNTs samples was performed using a coaxial dielectric barrier discharge (DBD) reactor in a tube–wire configuration. A quartz tube with an inner diameter of 6 mm and an outer diameter of 10 mm was used as the dielectric barrier. A coaxially inserted stainless-steel tube served as the high-voltage electrode, while aluminum foil wrapped around the outer surface of the quartz tube functioned as the grounded electrode. For each plasma treatment, 0.1 g of the FeNi-CNTs catalyst was loaded into the discharge zone, forming a fixed bed with a height of approximately 12 mm. By varying the plasma atmosphere, a series of plasma-modified catalysts were obtained. The resulting composite materials are denoted as FeNi-(x)P, where x represents the plasma atmosphere (Ar, N<sub>2</sub>, NH<sub>3</sub>, or 30%O<sub>2</sub>/Ar), indicating that plasma treatment was carried out after FeNi alloy nanoparticles had been successfully anchored onto the carbon nanotubes (FeNi-CNTs). The O<sub>2</sub> concentration of 30% was selected to achieve a balance between plasma stability, surface activation efficiency, and preservation of the carbon framework. At lower O<sub>2</sub>

concentrations, the plasma primarily induces physical etching with limited surface reconstruction, resulting in insufficient activation of FeNi active sites. In contrast, higher O<sub>2</sub> concentrations or stronger discharge conditions tend to cause excessive oxidation of the carbon nanotube support, which may deteriorate structural integrity and adversely affect electronic properties. Therefore, an O<sub>2</sub> concentration of 30% was adopted as an optimized condition in this study.

### 1.3 Electrochemical Setup and Electrode Preparation

The electrochemical performance of the as-prepared catalysts toward oxygen evolution reaction (OER) was evaluated using a CHI 660E electrochemical workstation at room temperature. Electrochemical measurements provide critical information on catalytic activity and stability, as well as interfacial processes such as charge transfer, adsorption, and mass diffusion at the electrode–electrolyte interface, which are essential for catalyst design and optimization. All electrochemical measurements were carried out in a standard three-electrode configuration. A rotating disk electrode (RDE) loaded with the catalyst was employed as the working electrode, while a platinum wire or carbon rod served as the counter electrode. A Hg/HgO electrode was used as the reference electrode. All electrodes were connected to the electrochemical workstation to enable precise potential control and accurate current measurement.

The working electrode was prepared as follows. A certain amount of catalyst was dispersed in a mixed solvent consisting of isopropanol, ultrapure water, and Nafion solution to form a catalyst ink. The suspension was ultrasonicated to obtain a homogeneous dispersion. Prior to catalyst loading, the glassy carbon electrode (diameter: 5 mm, geometric area: 0.196 cm<sup>2</sup>) was polished with Al<sub>2</sub>O<sub>3</sub> powder to achieve a mirror-like surface, followed by thorough rinsing with ultrapure water and drying under ambient conditions. Subsequently, 20 µL of the catalyst ink was drop-cast onto the clean glassy carbon surface in several steps and dried naturally. The catalyst loading was approximately 0.5 mg·cm<sup>-2</sup>. Commercial IrO<sub>2</sub> catalysts were prepared using the same procedure for comparison. Before electrochemical measurements, high-purity O<sub>2</sub> was purged into the 1.0 M KOH electrolyte for at least 30 min to ensure oxygen saturation. All measured potentials were converted to the reversible hydrogen electrode (RHE) scale according to the Nernst equation using the following relationship:

$$E_{VS, RHE} = E_{VS, Hg/HgO} + 0.059 \times \text{pH} + 0.098$$

### 1.4 Cyclic voltammetry (CV) measurements

CV measurements were performed by applying a triangular potential waveform to the working electrode, in which the potential was scanned from an initial value to a predefined vertex potential at a given scan rate and then reversed back to the initial potential, while recording the corresponding current response. For OER-related measurements, CV tests were carried out in 1.0 M KOH within the non-Faradaic potential region at different scan rates. The resulting capacitive currents were used

to determine the electrochemical double-layer capacitance ( $C_{dl}$ ), which was employed to qualitatively reflect the electrochemically active surface area (ECSA) of the catalysts.

### 1.5 Linear Sweep Voltammetry Measurements

Linear sweep voltammetry (LSV) was conducted by applying a continuously varying potential to the working electrode while recording the corresponding current response, yielding current-potential curves. This technique was used to evaluate catalytic activity and analyze reaction kinetics. For OER evaluation, catalytic activity was compared based on the overpotential ( $\eta$ ) required to reach a specific current density, where a lower overpotential indicates superior OER activity. In addition, Tafel slopes were derived from the LSV curves according to the Butler–Volmer relationship to evaluate the reaction kinetics. LSV measurements for OER were carried out at a scan rate of  $5 \text{ mV}\cdot\text{s}^{-1}$  within the potential range of 0–1.0 V (vs. RHE). The Tafel equation is expressed as:

$$\eta = a + b \times \log(j)$$

where  $a$  is the overpotential at a current density of  $1 \text{ A}\cdot\text{cm}^{-2}$ ,  $b$  is the Tafel slope, and  $j$  is the current density.

### 1.6 Electrochemical Impedance Spectroscopy

Electrochemical impedance spectroscopy (EIS) was employed to investigate the charge-transfer behavior of the catalysts by applying a small-amplitude alternating current (AC) signal over a wide frequency range. The impedance response was recorded as a function of frequency and analyzed to probe interfacial charge-transfer processes. In Nyquist plots, the intercept at the high-frequency region corresponds to the solution resistance, while the diameter of the semicircle reflects the charge-transfer resistance ( $R_{ct}$ ). The EIS data were fitted using ZView software to extract the corresponding equivalent circuit parameters.

### 1.7 Stability Tests

Electrochemical stability is a key metric for evaluating catalyst durability and long-term operational performance. In this work, the stability tests were performed using chronoamperometry at applied potentials of 1.51 V and 1.57 V vs. RHE for FeNi-O<sub>2</sub>P and FeNi-CNTs, respectively. All potentials were calibrated using a Hg/HgO (1 M KOH) reference electrode in 1 M KOH (pH 14).

### 1.8 Materials Characterization

The morphology and microstructure of the samples were characterized by scanning electron microscopy (SEM, TESCAN MIRA 3) and transmission electron microscopy (TEM, FEI Tecnai G2). SEM was employed to examine the surface morphology of the catalysts, while TEM and high-resolution TEM (HRTEM), combined with energy-dispersive X-ray spectroscopy (EDS), were used to investigate the particle size, crystalline structure, and elemental distribution. The crystal structure and phase composition of the samples were analyzed by X-ray diffraction (XRD) using a Bruker

D8 ADVANCE diffractometer with Cu K $\alpha$  radiation ( $\lambda = 0.15406$  nm), operated at 40 kV and 40 mA, over a  $2\theta$  range of 10–90°. X-ray photoelectron spectroscopy (XPS, Thermo Scientific K-Alpha) was conducted to determine the surface elemental composition and chemical states of the catalysts. Raman spectroscopy (Renishaw UK61M) was employed to evaluate the graphitization degree and structural disorder of the carbon framework.

## 2. Results

Tabel S1 Fe2p fine spectrum components of FeNi-CNTs and FeNi-O<sub>2</sub>P

Catalysts	Fe <sup>3+</sup>	Fe <sup>2+</sup>	Fe <sup>0</sup>
FeNi-CNTs	26.52%	47.27%	18.10%
FeNi-O <sub>2</sub> P	15.09%	52.22%	24.41%

Tabel S2 Ni 2p fine spectrum components of of FeNi-CNTs and FeNi-O<sub>2</sub>P

Catalysts	Ni <sup>3+</sup>	Ni <sup>2+</sup>	Ni <sup>0</sup> 2p	Fe/Ni
FeNi-CNTs	44.77%	24.54%	15.53%	1.43
FeNi-O <sub>2</sub> P	18.17%	33.60%	40.18%	1.38

Tabel S3 O 1s fine spectrum components of of FeNi-CNTs and FeNi-O<sub>2</sub>P

Catalysts	O1 (lattice oxygen)	O2 (hydroxyls)	O3 (H <sub>2</sub> O <sub>ads</sub> /C-O)	Concentration of O
FeNi-CNTs	19.11%	50.71%	30.18%	3.54%
FeNi-O <sub>2</sub> P	37.54%	41.99%	20.47%	6.30%

bel S3 O 1s fine spectrum components of of FeNi-CNTs and FeNi-O<sub>2</sub>P

Catalysts	O 1	O 2	O 3	O 含量
FeNi-CNTs	19.11%	50.71%	30.18%	3.54%
FeNi-O <sub>2</sub> P	37.54%	41.99%	20.47%	6.30%

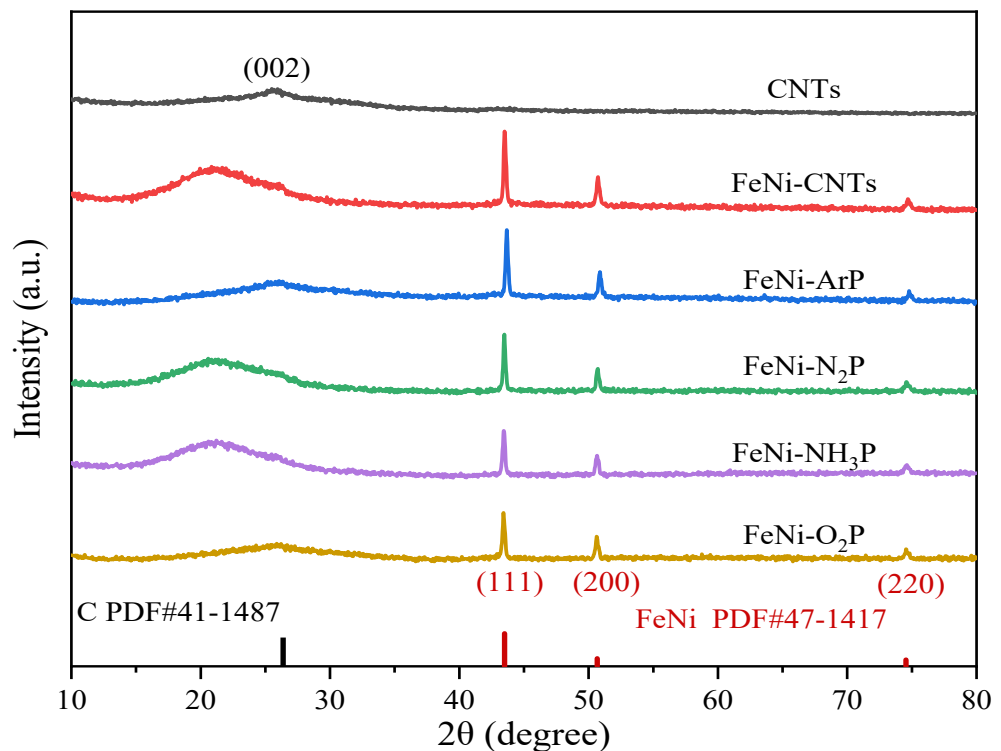


Figure S1 XRD patterns of CNTs, FeNi-CNTs, FeNi-ArP, FeNi-N<sub>2</sub>P, FeNi-NH<sub>3</sub>P, and FeNi-O<sub>2</sub>P

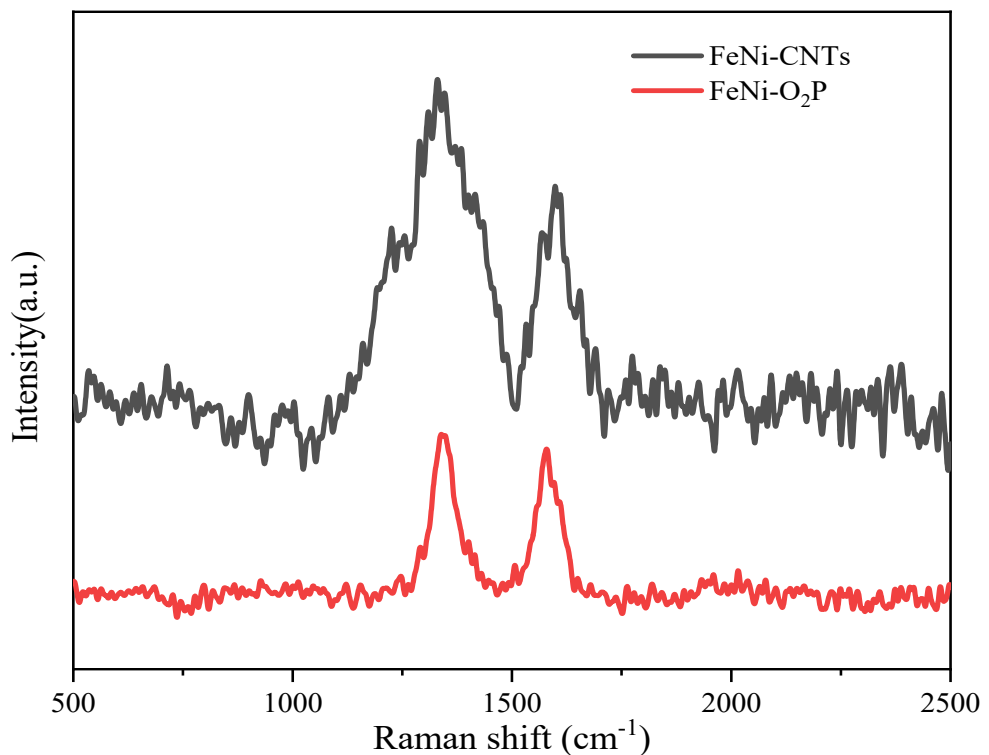


Figure S2 Raman diagram of FeNi-CNTs and FeNi-O<sub>2</sub>P

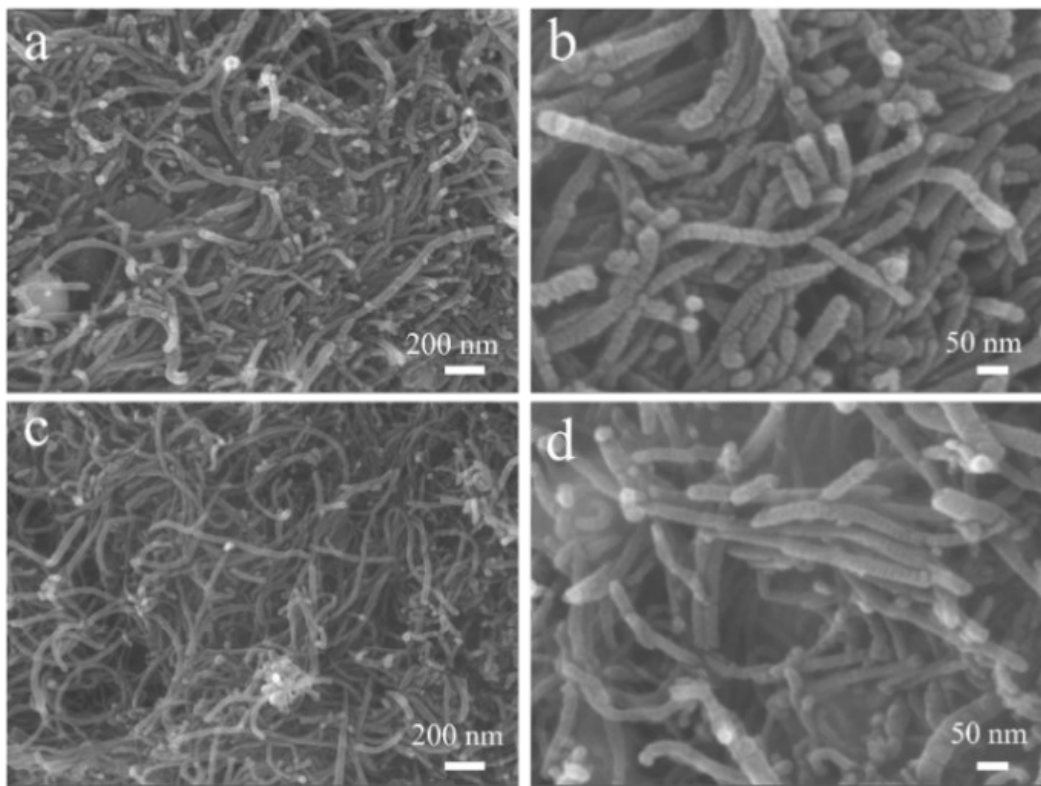


Figure S3 SEM images of FeNi-CNTs amplified at (a) 50,000 and (b) 200,000 multiples, and FeNi-O<sub>2</sub>P amplified at (c) 50,000 and (d) 200,000 multiples

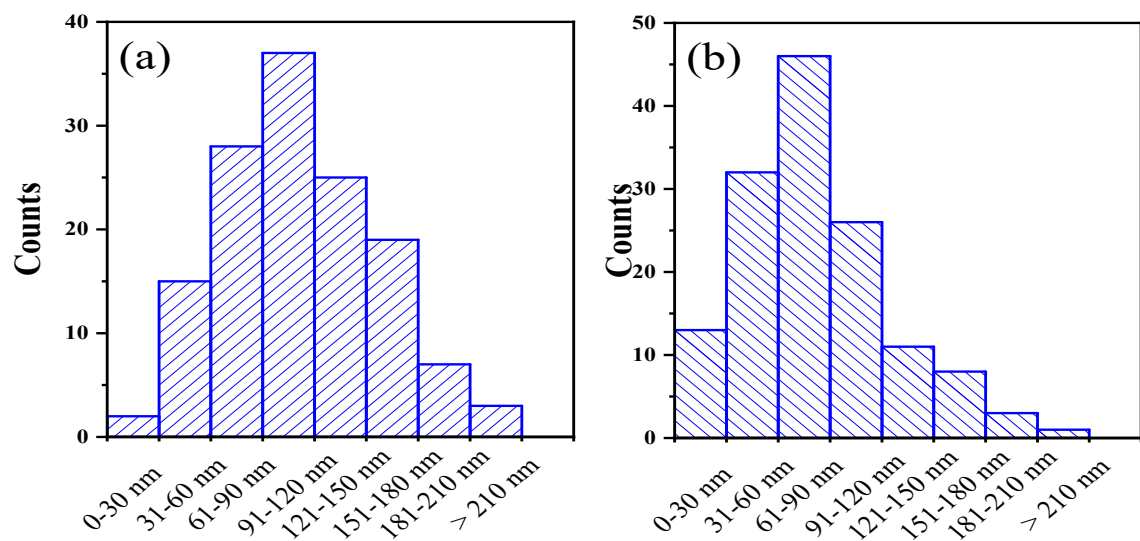


Figure S4 the particle size distribution histograms of (a) FeNi-CNTs and (b) FeNi-O<sub>2</sub>P

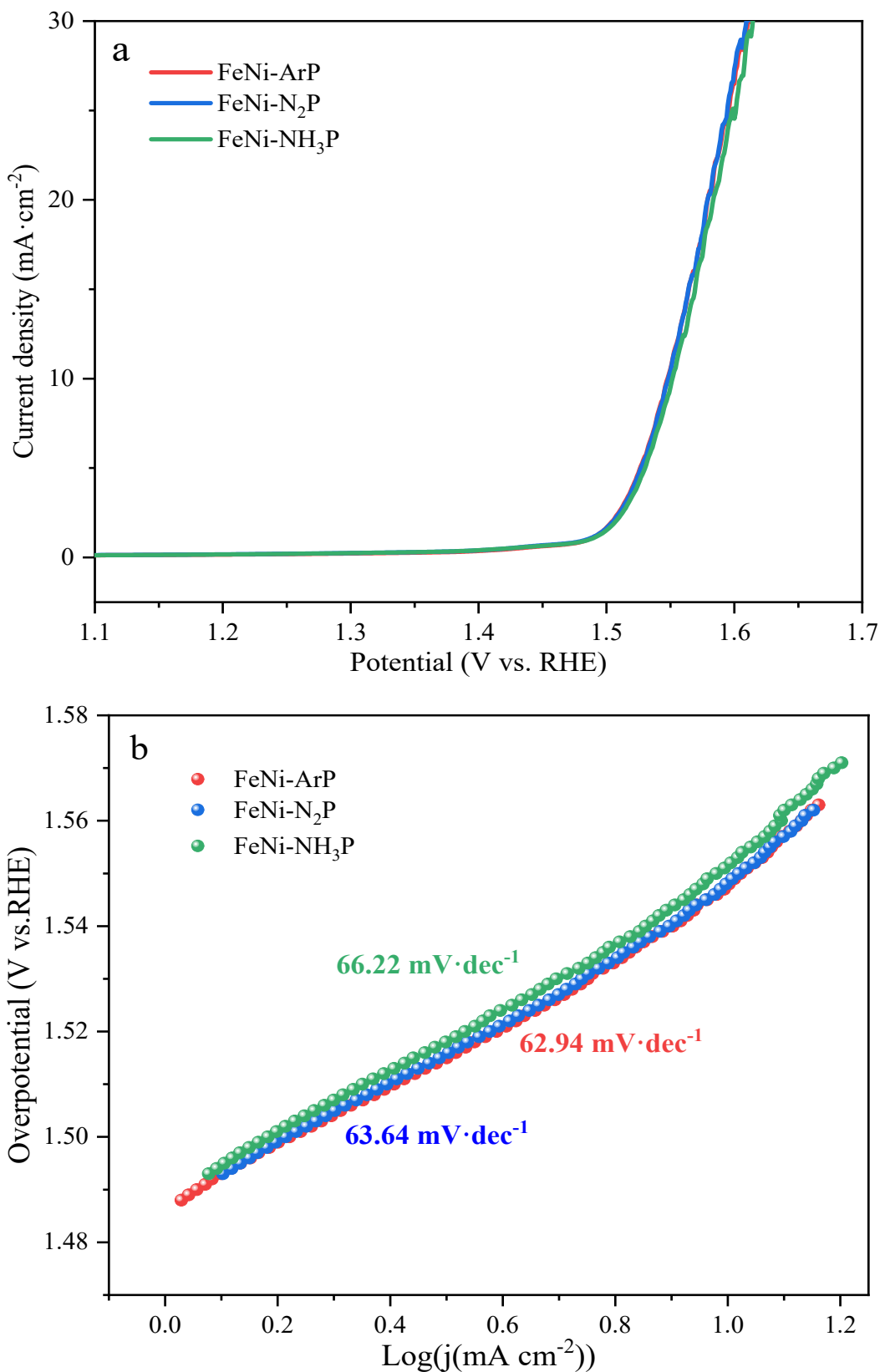


Figure S5 (a) LSV curve and (b) Tafel slope of OER reaction of FeNi-ArP, FeNi-N<sub>2</sub>P, and FeNi-NH<sub>3</sub>P

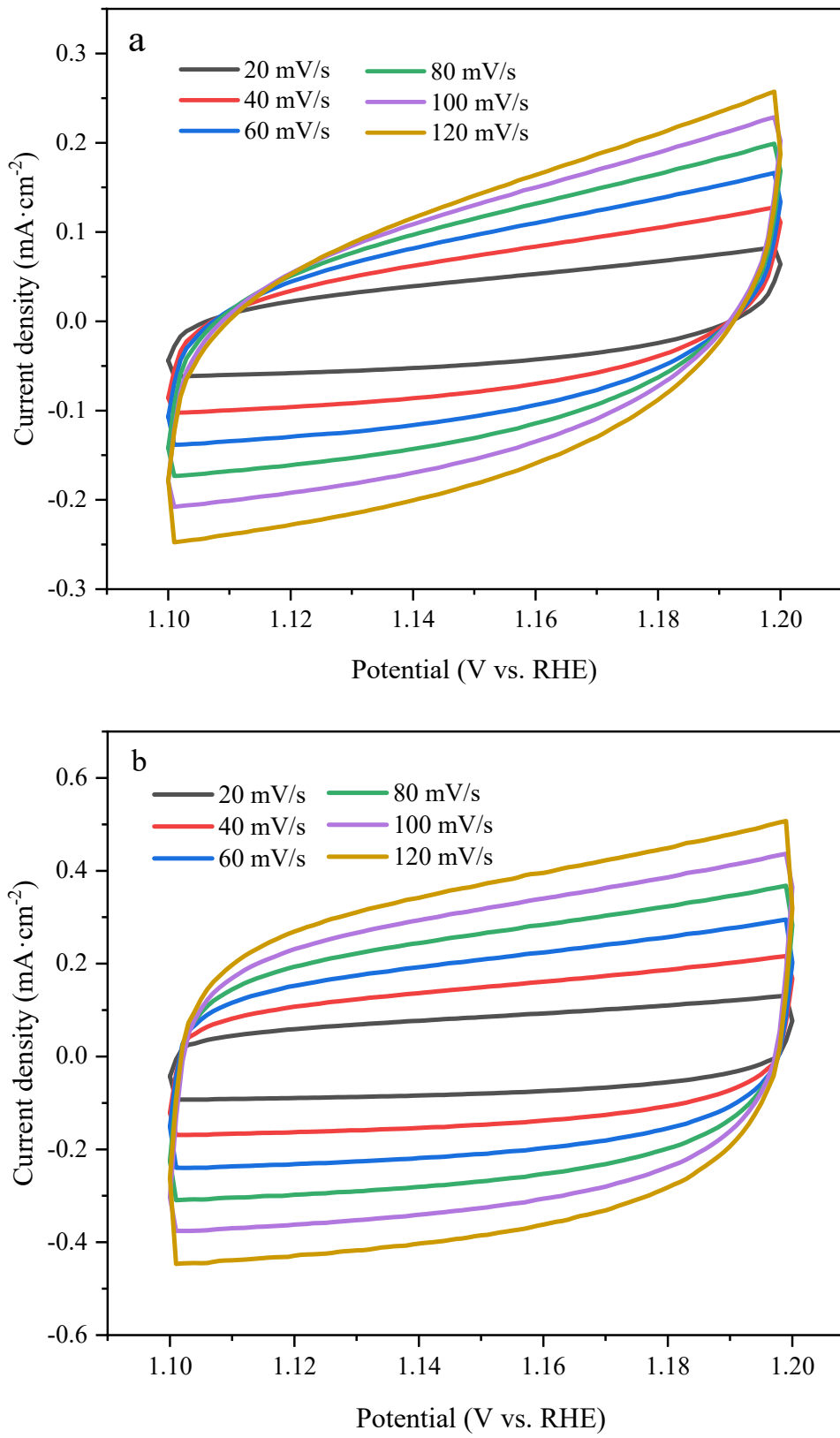


Figure S6 CV curves of (a) FeNi-CNTs and (b) FeNi-O<sub>2</sub>P at different scanning rates in the voltage range of 1.1 V to 1.2 V